https://doi.org/10.5194/egusphere-2026-5279
Preprint. Discussion started: 3 September 2026
© Author(s) 2026. CC BY 4.0 License.

Shifts in rain-on-snow occurrence in northwestern Eurasia and their connection to Arctic sea ice loss

Gaëlle Veyssière[1], Julienne Stroeve[2,3,4], Ran Tao[2], Bruce C. Forbes[5]

1 British Antarctic Survey, High Cross, Madingley Road, Cambridge CB3 0ET, United Kingdom

2 Alfred Wegener Institute, Helmholtz Centre for Polar and Marine Research, Am Handelshafen 12, 27570 Bremerhaven, Germany

3 Canada 150 Research Chairs Program, Centre for Earth Observation Science, University of Manitoba, 535 Wallace Building, 125 Dysart Rd., Winnipeg, MB R3T 2N2, Canada

4 National Snow and Ice Data Center, Cooperative Institute for Research in Environmental Sciences (CIRES), 449 UCB, University of Colorado Boulder, Boulder, CO 80309-0449, USA

5 Arctic Centre, University of Lapland, Pohjoisranta 4, FI-96200 Rovaniemi, Finland

Correspondence: G. Veyssière, gaevey@bas.ac.uk

Abstract

This study explores precipitation, rain-on-snow (ROS) events and subsequent refreezing across northwestern Eurasia, and their relationship with Arctic sea ice. Daily outputs from nine CMIP6 models were analysed for 2015-2100 under three emission scenarios. ROS events were detected using precipitation, temperature, and snow cover after bias correction, and refreezing was identified when sub-freezing temperatures were found within four days after ROS. We find increasing winter precipitation across northwestern Eurasia, dominated by a shift towards more rainfall. The shift from snow to rainfall is more pronounced where temperatures remain near 0°C, leading to changes in ROS frequency and timing under higher emissions. ROS events followed by refreezing occur less frequently than the total ROS events but indicate conditions favourable for ice-layer formation within the snowpack. The greatest changes occur between 55°N and 70°N, while northern regions remain less affected. ROS timing shifts from spring peaks towards later winter and early spring; at lower latitudes, the spring peak weakens as snow cover becomes less persistent. The Barents-Kara sea ice concentration anomalies are negatively correlated with accumulated precipitation and rainfall. Detrending of the correlations shows that the common long-term trend partly drives this relationship, but negative correlations between sea ice concentration anomalies and rainfall remain in several cases. Future ROS changes are driven mainly by increased rainfall rather than by total precipitation alone, while subsequent refreezing remains dependent on sub-freezing conditions following rainfall. The projected shifts in ROS timing and refreezing may affect snow conditions, socio-ecological systems, and infrastructure across northwestern Eurasia.

1 Introduction

The Arctic has warmed rapidly in recent decades, with warming at high latitudes exceeding the global average (Serreze and Barry, 2011; Rantanen et al., 2022). This Arctic amplification has been accompanied by widespread sea ice decline, shorter snow cover duration, and increases in precipitation and atmospheric moisture (Döscher et al., 2014; Box et al., 2019; Dauginis and Brown, 2021). One consequence of this warming has been a shift in the precipitation regime. As temperatures increase, a larger fraction of cold-season precipitation falls as rain rather than snow, particularly when temperatures fluctuate around the freezing point (Bintanja and Andry, 2017; McCrystall et al., 2021). Because the precipitation phase controls snow accumulation and surface energy exchange, even small temperature changes can have disproportionate effects on hydrological processes (Adam et al., 2009; DeWalle and Rango, 2008). This shift leads to the potential for winter rain-on-snow (ROS) events, which arise when rainfall

© Author(s) 2026. CC BY 4.0 License.

occurs over an existing snowpack. Some ROS events may then be followed by refreezing if temperatures fall below 0°C in the following days. ROS events and subsequent refreezing are frequently observed in high-latitude and maritime regions, such as Fennoscandia and northern Eurasia (Ye et al., 2008; Cohen et al., 2015; Pall et al., 2019). They are typically associated with warm-air intrusions linked to cyclonic activity, potentially followed by a return to freezing conditions (Rennert et al., 2009; Hansen et al., 2014). When rain infiltrates the snowpack and refreezes, ice layers can form within the snowpack or at its base, altering snow structure, density, and thermal properties (Putkonen and Roe, 2003; Grenfell and Putkonen, 2008). ROS events affect both hydrological and ecological systems. They can accelerate snowmelt, reduce water storage, and modify the timing and magnitude of runoff (McCabe et al., 2007; Rennert et al., 2009). The formation of ice layers can also influence ground thermal regimes and permafrost conditions (Putkonen and Roe, 2003; Romanovsky et al., 2010). Additionally, ice crusts can limit access to vegetation, contributing to large-scale mortality in reindeer and caribou populations, with widespread impacts on ecosystems and local livelihoods (Bartsch et al., 2010, 2023; Forbes et al., 2016; Serreze et al., 2021; Laptander et al., 2024).

Changes in Arctic precipitation have been linked to declining sea-ice levels. The loss of sea ice exposes open water, enhancing heat and moisture fluxes to the atmosphere and increasing lower-tropospheric humidity (Screen and Simmonds, 2010; Bintanja and Selten, 2014; Boisvert and Stroeve, 2015). These processes favour precipitation and increase the likelihood of rainfall during the cold season (Deser et al., 2010; Bintanja and Andry, 2017). Sea-ice variability is coupled to changes in atmospheric circulation (Walsh and Johnson, 1979; Vihma, 2014). Reduced winter sea ice can also influence cyclone development and cyclone-associated precipitation over the Arctic Ocean (Crawford et al., 2022). Atmospheric circulation variability, in turn, has an important influence on precipitation across Arctic Fennoscandia (Marshall et al., 2020). Northern Fennoscandia is a key region in which these processes interact. It is at the intersection between maritime and continental climate regimes and is greatly influenced by conditions in the Barents and Kara seas. Sea ice variability, combined with a complex topography, both contribute to strong spatial variability in temperature and precipitation (Smedsrud et al., 2013; Marshall et al., 2018). Time series from 1914-2013 have indicated that the region experienced significant warming, particularly in autumn and spring, together with an increase in precipitation and a shortening of the colder season (Kivinen et al., 2017). The future evolution and spatial distribution of ROS events in this region, however, remain uncertain despite more recent attention. In particular, it remains unclear how precipitation phase and snow availability will interact across latitudes, and how Barents-Kara sea ice loss relates to precipitation and ROS occurrence over northwestern Eurasia. While previous studies have highlighted links between large-scale atmospheric circulation and ROS variability (Cohen et al., 2015), the future evolution of these relationships under continued warming is unclear. This study examines future changes in ROS across northwestern Eurasia and their relationship with Barents-Kara sea ice concentration.

2 Methods and data

2.1 Climate model data

A subset of models from the sixth phase of the Coupled Model Intercomparison Project (CMIP6; Eyring et al., 2016) were considered. These models were selected based on the availability of the variables required for the analysis. Nine models were retained: BCC-CSM2-MR, CanESM5, CMCC-ESM2, EC-Earth3-Veg, IPSL-CM6A-LR, MIROC6, MPI-ESM1-2-HR, MPI-ESM1-2-LR, and MRI-ESM2-0. To ensure comparability and avoid differences arising from ensemble size, only the first realisation (ensemble member r1i1p1f1) from each model was used in the analysis. Key variables relevant to precipitation phase and cryospheric processes were selected: total precipitation (pr), minimum (tasmin), and maximum (tasmax) near-surface air temperatures, sea ice concentration (siconc), and snow cover fraction (snc). All variables were extracted at daily resolution. This temporal resolution was used to capture the variability of mixed-phase precipitation, ROS events, and subsequent refreezing, which are frequently associated with transient synoptic conditions (Hansen et al., 2014; Serreze et al., 2021). Future projections were analysed using three Shared Socioeconomic Pathways (SSPs), representing a range of greenhouse gas emission scenarios and increases in global temperature (O'Neill et al., 2016), SSP1-2.6, SSP2-4.5, and SSP5-8.5 reflecting

https://doi.org/10.5194/egusphere-2026-5279
Preprint. Discussion started: 3 September 2026
© Author(s) 2026. CC BY 4.0 License.

low, intermediate and high emissions, respectively. The three scenarios correspond to approximately +1.4 to +1.8°C, +2.1 to +3.5°C, and +3.3 to +5.7°C global mean temperature increases by the end of the century, respectively, relative to pre-industrial levels (IPCC, 2021). Furthermore, we considered the period of 2015-2100, as this time frame allows for the assessment of long-term trends and changing variability in precipitation, temperature extremes, and sea ice. By combining multiple models and scenarios, this study captures a range of potential climate responses and robust signals in precipitation phase changes and their links to sea ice variability.

2.2 Area of study

The area used in terms of ROS events analysis covered the northwestern Eurasian land, defined here as the region spanning 55°N to 78°N and 0°E to 90°E. This domain includes Norway, Sweden, Finland, and parts of northwestern Russia and West Siberia, and encompasses a wide range of climatic conditions from maritime environments along the Norwegian coast to more continental regimes further inland. The region is characterised by strong gradients in temperature and precipitation, which are influenced by North Atlantic storm tracks, complex topography, and proximity to Arctic Ocean regions.

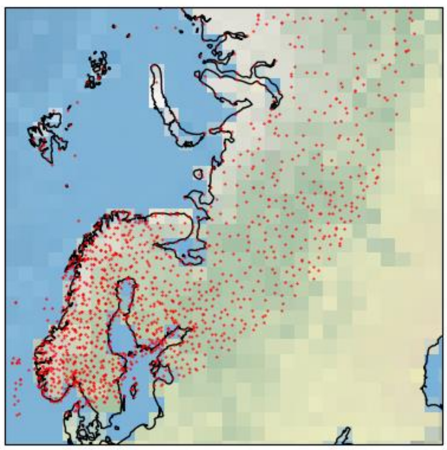

Figure 1. Map of the study region together with the location of the stations (red dots) used to produce the gridded station data applied during the bias correction. On average 450 stations per year for the period 1981-2011.

The selection of this domain was motivated by its climatic, socio-economic and ecological relevance and the availability of high-quality gridded observational datasets. Northern Fennoscandia has a relatively large station network (Fig. 1) compared with other Arctic regions, providing the observational coverage needed to produce gridded datasets for bias correction. Distribution-based bias correction relies on such observational references to adjust the statistical properties of climate model simulations (Gudmundsson et al., 2012; Chen et al., 2013). In addition to the regional land-based domain considered for ROS frequency, sea-ice conditions were included in the analysis to evaluate their potential relationship with precipitation variability. Sea ice concentration (SIC) was considered over the Barents and Kara seas. These seas are of particular interest because of their rapid warming and pronounced decrease in winter sea ice, which have been shown to influence atmospheric circulation, moisture transport, and precipitation patterns over northern Europe (Smedsrud et al., 2013; Screen and Simmonds, 2010).

https://doi.org/10.5194/egusphere-2026-5279
Preprint. Discussion started: 3 September 2026
© Author(s) 2026. CC BY 4.0 License.

2.3 Bias correction and preprocessing

Climate model outputs are known to display systematic biases in key variables such as precipitation and temperature, arising from limitations in the representation of processes including convection, cloud formation, and land-atmosphere interactions (Flato et al., 2013; Cannon et al., 2015). These biases can affect precipitation intensity, frequency, and phase both spatially and temporally, and therefore need to be addressed before impact-oriented analyses. Bias correction techniques are commonly applied as a post-processing step to adjust model outputs so that their statistical properties are consistent with observations while preserving the projected climate change signal (Teutschbein and Seibert, 2012). Daily precipitation and minimum/maximum near-surface temperature were bias-corrected using a distribution-based approach following the semi-parametric quantile mapping (SPQM) method described in Rajulapati and Papalexiou (2023). Such methods adjust the cumulative distribution function of the model simulations to match the observations and are used because they allow to correct biases across the full range of values, including extremes (Gudmundsson et al., 2012; Cannon et al., 2015). Applying the same bias-correction framework to temperature and precipitation maintains consistency among the corrected variables, an important factor as small temperature biases around the freezing point can lead to substantial errors in partitioning rainfall and snowfall.

SIC and snow cover fraction were bias-corrected using a dynamical statistical approach modified from the MARVIC bias correction method (Melia et al., 2015; Crawford and Stroeve, 2023), with a dynamic mean/variance correction after regridding to the NSIDC Polar Stereographic North projection at 25 km resolution. Sea ice concentration was adjusted to match observed climatological distributions while preserving temporal variability and long-term trends, with values constrained to the physical range of 0-100 % (Crawford and Stroeve, 2023). For snow cover, the fraction was first converted to a binary representation of snow, with grid cells considered snow-covered when the snow cover fraction exceeded 0.5. The resulting product was then bias-corrected against satellite-derived snow extent climatology for 1999-2012. This correction was used to reduce model biases in snow cover occurrence and seasonality. All variables were processed at daily temporal resolution to identify short-duration events such as rainfall on snow-covered surfaces and subsequent refreezing. The processed datasets were then all reprojected on the NSIDC Polar Stereographic North projection (25 km resolution) to ensure spatial consistency across models and variables while preserving large-scale spatial patterns.

2.4 Definition of events

The variables considered were used to derive the precipitation phase and identify ROS events over the study area. Daily precipitation and temperature data were analysed together to distinguish between rainfall and snowfall conditions. The mean daily air temperature was estimated as the average of the minimum and maximum near-surface temperatures. Precipitation was classified as rainfall when the mean daily temperature exceeded 0°C and as snowfall otherwise. This threshold-based approach is commonly applied in large-scale studies, although it simplifies the phase partitioning processes that depend on the vertical atmospheric structure and on sub-daily temperature variability (Knowles et al., 2006; Harpold et al., 2017). In particular, the use of daily data does not resolve diurnal phase changes, and short periods of rainfall or refreezing within a day may be missed. However, daily data were used because they are available consistently across the CMIP6 models and scenarios analysed here, and because they allow ROS events to be identified over long time periods using the same criteria for all models. The snow cover conditions were derived from the snow cover fraction variable. For this analysis, snow presence was defined using a binary method, where a grid cell was considered snow-covered when the snow cover fraction exceeded 50%, allowing for consistent identification of snow-covered conditions across models. ROS events were defined based on three conditions simultaneously met: (i) daily precipitation occurred (pr > 0), (ii) mean daily temperature exceeded 0°C, and (iii) snow was present at the surface, allowing rainfall on an existing snowpack. Furthermore, ROS events followed by refreezing were identified as the subset of ROS events for which mean daily air temperature fell below 0°C on at least one of the next four days, with potential formation of an ice layer within the snowpack. Daily event frequency within latitude bands was calculated as the fraction of land grid cells meeting the ROS event (and followed by refreezing) criteria on each winter day and then averaged across the winters in each selected period.

© Author(s) 2026. CC BY 4.0 License.

SIC was analysed separately to investigate its relationship with precipitation variability. Regional SIC averages were calculated over the Barents and Kara seas while land-mean accumulated precipitation and rainfall were averaged over all land grid cells within the full study area (see Sect. 2.2). Additionally, SIC anomalies were calculated as the difference between the projected SIC and reference climatology for the period 1981-2010, derived from satellite observations, allowing us to assess variations from the baseline conditions as well as comparisons across models and scenarios.

2.5 Statistical analysis

Extreme precipitation and rainfall events were defined using the 95th-percentile thresholds per grid cell for each scenario over all complete winters from 2015 to 2099. For total precipitation, the percentile was calculated based on all winter days over land, including days without precipitation while for rainfall, the percentile was calculated from rainy days only, defined as days with precipitation > 0 and mean daily temperature > 0°C. This accounts for spatial differences in the precipitation distribution and provides a relative measure of extremes that is comparable across regions with different initial conditions (Alexander et al., 2006; Donat et al., 2013), defined as the number of extreme event days for each winter season. The winter period was defined as the extended cold season from 1 October to 30 April, encompassing both the core winter months and transitional months when temperatures frequently fluctuate around the freezing point. This extended season is particularly relevant for analysing rainfall, ROS and ROS followed by refreezing processes, which are more likely to occur during the shoulder months. Temporal changes in the frequency of extreme precipitation and rainfall events were assessed by calculating linear trends in the annual number of event days over the full analysis period for each scenario. Trends were estimated using ordinary least squares regression and expressed as changes in the number of event days per winter per decade. Correlations between precipitation/rainfall and SIC anomalies were calculated first. We then repeated the analysis after removing the linear trend from each time series to assess how much of the relationship remained after detrending. For each scenario, and for the full winter season and individual shoulder months, linear trends were fitted to and removed from the Barents-Kara SIC anomaly, land-mean accumulated precipitation, and land-mean accumulated rainfall time series. Pearson correlations were calculated from the resulting residuals. These correlations were used as a sensitivity analysis and were not interpreted as evidence of causality.

3 Results

3.1 Future changes in precipitation and rainfall

Across all scenarios, winter precipitation increases over the study region, with the magnitude of change tied to the emissions pathway. Trends in extreme precipitation (above the 95th percentile) show a consistent increase over most of the area of interest (Fig. 2). These increases remain relatively small and spatially uniform under SSP1-2.6, but intensify under SSP2-4.5, adding between 1 and 2 extreme precipitation events per winter per decade across nearly the entire study region. SSP5-8.5 produces the largest changes, with the number of extreme precipitation days increasing across almost the entire region and reaching up to 3 additional events per winter per decade over land adjacent to the Barents and Kara seas. Trends in extreme rainfall days are smaller in magnitude but follow a similar spatial pattern, with limited changes under SSP1-2.6 and more widespread increases under SSP2-4.5 and especially SSP5-8.5. Under SSP5-8.5, extreme rainfall day frequency increases across coastal Fennoscandia and western Russia, exceeding 1.5 additional days per winter per decade in some areas.

https://doi.org/10.5194/egusphere-2026-5279
Preprint. Discussion started: 3 September 2026
© Author(s) 2026. CC BY 4.0 License.

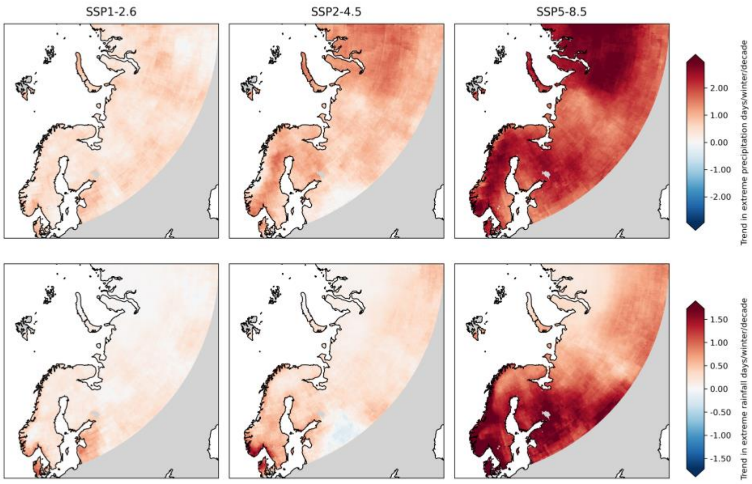

Figure 2. Spatial trends in extreme precipitation (top row) and extreme rainfall (bottom row) days per winter per decade, computed for the period 2015–2100. Three SSPs are depicted: SSP1-2.6 (left column), SSP2-4.5 (middle column), and SSP5-8.5 (right column).

3.2 Changes in ROS seasonality and latitudinal variability

The seasonal distribution of ROS changes over the century, with the clearest changes under SSP2-4.5 and SSP5-8.5 (Figs. 3–5, left panels). In 2025-2035, ROS events are concentrated mainly during spring between 55° N and 70°N, with low frequency during December-February. Under SSP5-8.5, the spring ROS frequency peaks at 0.37 at 55-60°N, 0.37 at 60-65°N and 0.31 at 65-70°N. By 2089-2099, ROS events occur over a larger part of winter and the spring maximum is lower and occurs earlier. At 55-60°N under SSP5-8.5, the 0.35 April peak evident in 2025-2035 is replaced by lower frequencies spread across January-March. At 60-65°N, the SSP5-8.5 frequency reaches 0.16 in mid-March by the end of the century, while the mid-April frequency falls from 0.36 in 2025-2035 to 0.02 in 2089-2099. A similar change occurs at 65-70° N, where the late-spring maximum of 0.31 in the early period is replaced by a broader March-April period, reaching 0.18 in late March under SSP5-8.5.

The same redistribution is present under SSP2-4.5, although it is weaker than under SSP5-8.5. At 55-60°N, the ROS frequency on 1 April decreases from 0.28 in 2025-2035 to 0.07 in 2089-2099, while the January frequency increases from values close to zero to 0.02. At 60-65°N, the frequency on 15 April decreases from 0.31 to 0.09 between the early and late periods, and ROS events become more frequent during March. At 65-70°N, the early-period spring maximum of 0.28 falls to 0.12 by the end of the century and occurs earlier in the season. Changes under SSP1-2.6 are smaller and the spring concentration remains more evident. North of 70°N, ROS frequencies remain low throughout the three periods. The contrast is strongest at 70-75°N, where events are mainly restricted to autumn, while mean frequencies at 75-78°N remain close to zero during most of the cold season.

ROS events followed by refreezing (Figs. 3-5, right panels) show a similar seasonal change, but at lower frequencies. At 55-60°N under SSP5-8.5, the maximum frequency decreases from 0.08 in late March in 2025-2035 to 0.04 in early January in 2089-2099, indicating both a reduction in the seasonal maximum and a shift away from the spring peak. At 60-65°N, the early-period maximum is 0.12 under SSP5-8.5 and 0.14 under SSP2-4.5; by 2089-2099 the corresponding maxima are 0.05 for both pathways, with events spread more broadly from winter into early spring. The same behaviour is visible at 65-70°N, although the spring signal persists for longer than at the lower latitudes. Overall, both ROS and ROS followed by refreezing shift from pronounced spring peaks towards a broader winter occurrence, while spring frequencies decrease at the lower latitudes.

https://doi.org/10.5194/egusphere-2026-5279
Preprint. Discussion started: 3 September 2026
© Author(s) 2026. CC BY 4.0 License.

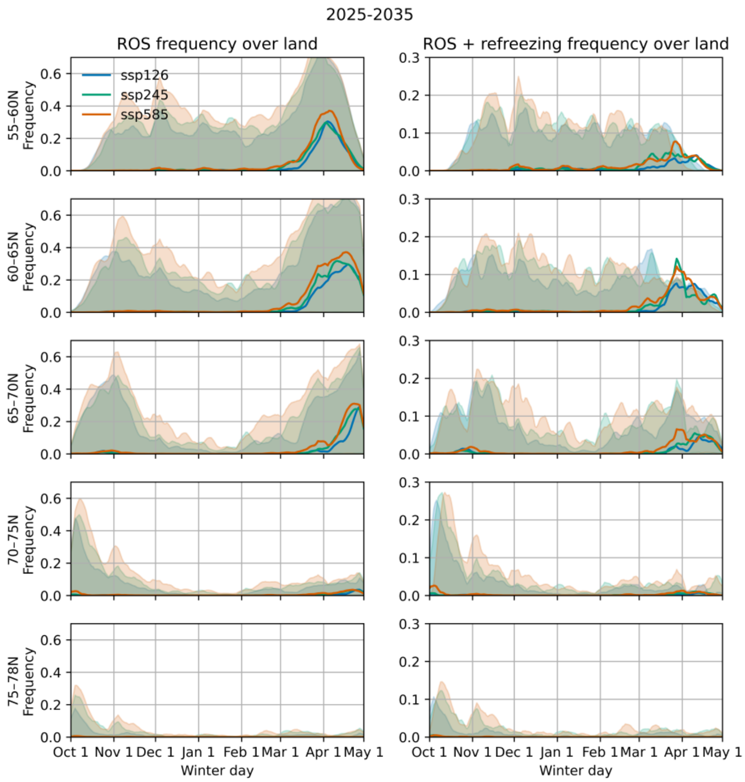

Figure 3. ROS events (left column) and ROS followed by refreezing (right column) for the period 2025-2035. Frequency is defined as the fraction of land grid cells within each latitude band experiencing the event on a given winter day, averaged across the winters in the period. Lines are calculated from ensemble-mean input fields, and the shaded envelope spans frequencies obtained from input fields corresponding to the ensemble mean plus or minus one standard deviation. Results are shown for SSP1-2.6 (blue), SSP2-4.5 (green), and SSP5-8.5 (orange), and for five latitude bands from top to bottom: 55°-60°N, 60°-65°N, 65°-70°N, 70°-75°N, and 75°-78°N.

© Author(s) 2026. CC BY 4.0 License.

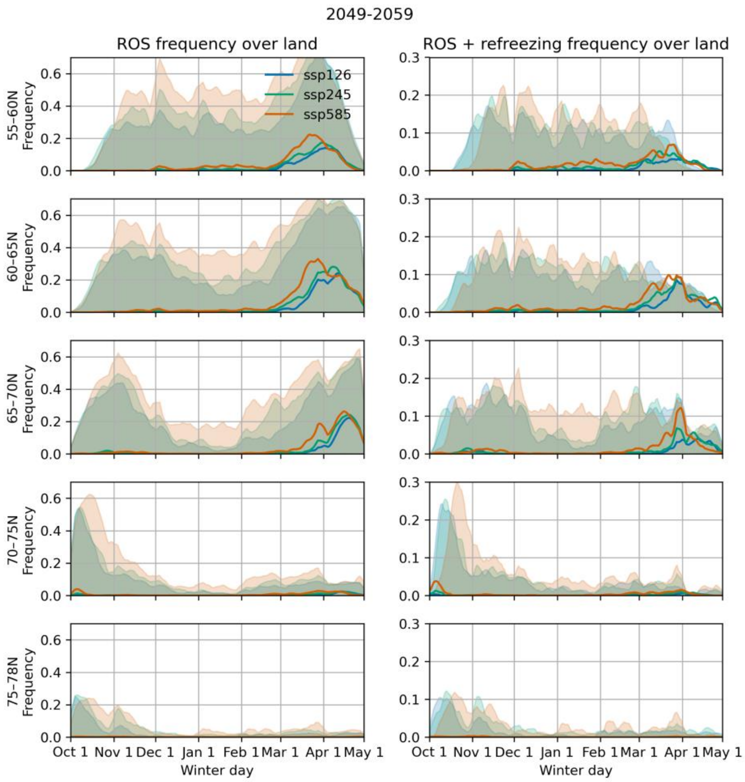

Figure 4. Same as Figure 3, for the period 2049-2059.

https://doi.org/10.5194/egusphere-2026-5279
Preprint. Discussion started: 3 September 2026
© Author(s) 2026. CC BY 4.0 License.

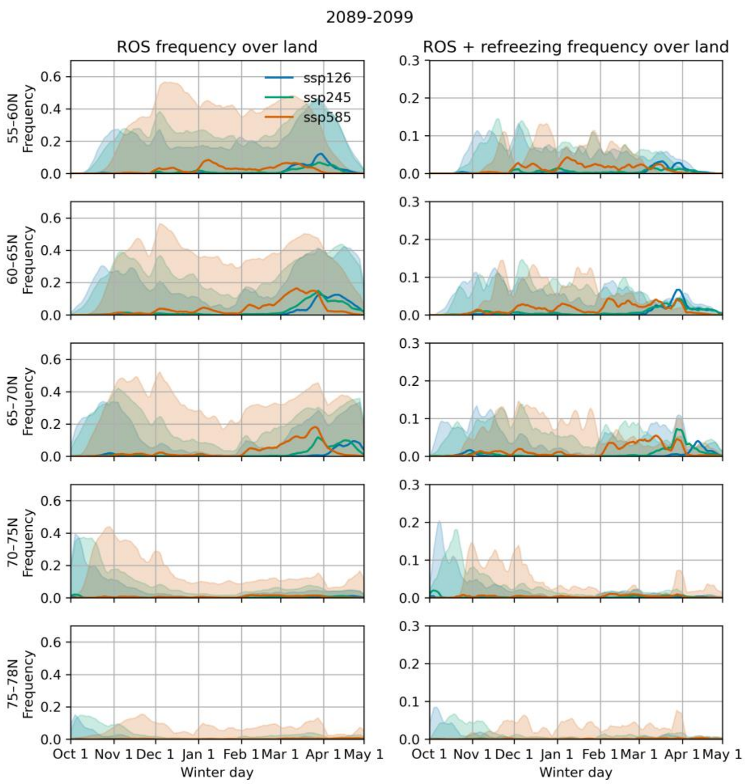

Figure 5. Same as Figure 3 and 4, for the period 2089-2099.

3.3 Evolution of accumulated precipitation/rainfall and relationship with sea ice concentration

Throughout the century, land-mean winter precipitation and rainfall increase, ranging from modest gains under SSP1-2.6 to stronger trends under SSP2-4.5 and the largest increases under SSP5-8.5 (Fig. 6). Near the start of the projections, land-mean total winter precipitation is approximately 100 mm and rainfall about 25-30 mm across the three scenarios. By the 2090s, total precipitation reaches roughly 110 mm under SSP1-2.6, 115 mm under SSP2-4.5, and 145 mm under SSP5-8.5; corresponding rainfall amounts are about 30 mm, 40-45 mm, and 75-80 mm. Overall, rainfall increases faster than total precipitation, indicating a shift from snowfall to rainfall. By the end of the century, this shift is particularly pronounced under SSP5-8.5, where rainfall accounts for a larger share of winter precipitation, increasing from ~30% early in the century to ~53% in the 2090s. Over the same period, winter Barents-Kara SIC anomalies become increasingly negative, reaching roughly -45%, -50%, and -65% by the 2090s under SSP1-2.6, SSP2-4.5, and SSP5-8.5, respectively. The correlations between SIC anomaly and winter precipitation are -0.69, -0.84, and -0.94, while the correlations with rainfall are stronger at -0.80, -0.91, and -0.95, respectively for each scenario.

The monthly analysis focuses on October, November, March and April, which represent the shoulder months, when changes in precipitation phase are particularly relevant to ROS occurrence (Fig. 7). In October and November, accumulated precipitation and rainfall increase with time, although rainfall shows consequent interannual variability. These changes are more pronounced in March and April, particularly under SSP2-4.5 and SSP5-8.5, when rainfall increases more strongly than total precipitation. The SIC anomaly is negatively correlated with total precipitation in all four months, showing sea ice loss together with an increase in precipitation. Under SSP1-2.6, the correlations

https://doi.org/10.5194/egusphere-2026-5279
Preprint. Discussion started: 3 September 2026
© Author(s) 2026. CC BY 4.0 License.

range from -0.36 in March to -0.47 in April; under SSP2-4.5, from -0.49 in October to -0.62 in November; and under SSP5-8.5, from -0.60 in October to -0.81 in April. The relationship is stronger for rainfall in most cases. Correlations range from -0.52 in November to -0.64 in April under SSP1-2.6, from -0.66 in October to -0.79 in March under SSP2-4.5, and from -0.68 in October to -0.92 in both March and April under SSP5-8.5.

Detrending weakens the correlations, showing that part of the relationship with Barents-Kara SIC is associated with the shared long-term trends (Fig. 8). In some cases, the negative relationship is no longer present, particularly for total precipitation under SSP5-8.5 and for several autumn correlations. However, the relationship remains more evident for rainfall. For the full winter, detrended rainfall correlations remain at -0.44 under SSP1-2.6 and -0.42 under SSP2-4.5. Negative correlations are also retained in March and April under all three scenarios, reaching -0.35 in April under SSP1-2.6, -0.42 in April under SSP2-4.5, and -0.34 in March under SSP5-8.5. The persistence of these negative correlations, particularly during the late-winter and spring shoulder period, indicates that the association between lower Barents-Kara SIC and higher rainfall is not solely due to their common long-term trends.

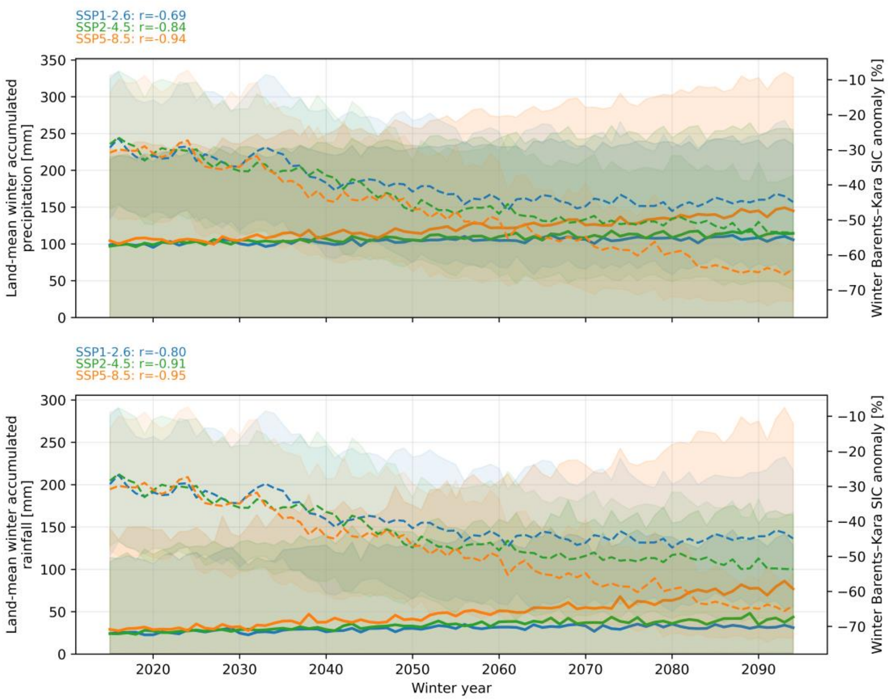

Figure 6. Land-mean accumulated precipitation (top) and rainfall (bottom) over the winter season, with standard deviation shown by the shaded area, and Barents-Kara sea ice concentration (SIC) anomaly shown by dotted lines for the three SSPs (blue: ssp126, green: ssp245, and orange: ssp585). The correlation coefficients between precipitation/rainfall and Barents-Kara SIC anomalies for all scenarios are given above the panels.

https://doi.org/10.5194/egusphere-2026-5279
Preprint. Discussion started: 3 September 2026
© Author(s) 2026. CC BY 4.0 License.

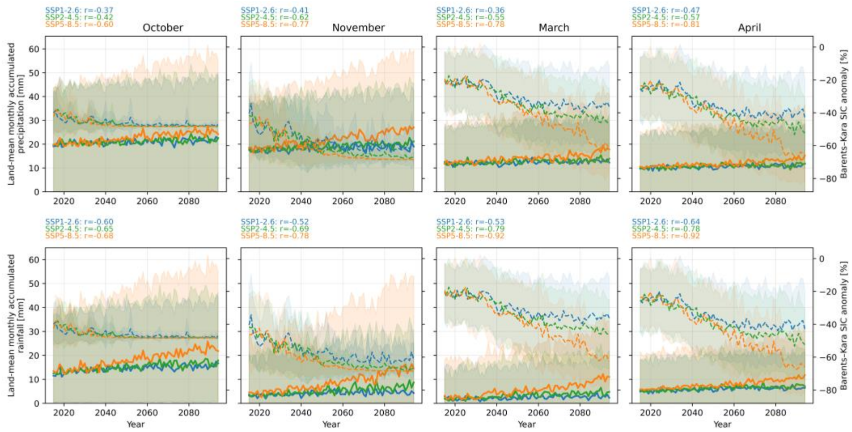

Figure 7. Same as Figure 6 for October, November, March, and April.

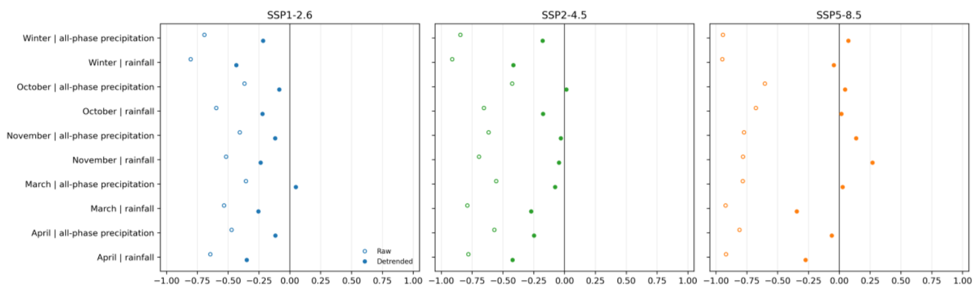

Figure 8. Raw and detrended Pearson correlations between Barents-Kara SIC anomalies and land-mean accumulated precipitation/rainfall. The correlations are shown separately for each scenario (by panels), and for the full winter season, October, November, March, and April (y-axis). Open circles show the raw correlations, while filled circles show correlations after removing the linear trend from both the SIC anomaly and precipitation/rainfall time series. Negative values indicate that lower SIC is associated with higher land-mean accumulated precipitation or rainfall; positive detrended values indicate a reversal of this relationship after linear trend removal.

4 Discussion

4.1 Changes in ROS occurrence and seasonality

The projected changes in ROS are closely linked to the increasing proportion of winter precipitation falling as rain. Total precipitation increases in all three scenarios, but the increase in rainfall is much stronger, particularly under SSP5-8.5. As winter temperatures rise, precipitation is more likely to fall as rain when temperatures are close to 0°C (Berghuijs et al., 2014; Harpold et al., 2017). This is particularly important between about 60°N and 70°N, where snow remains on the ground for much of the winter but rainfall becomes increasingly frequent. Relatively small changes in temperature can produce a noticeable change in precipitation phase in such regions (Barnett et al., 2005). Further north, temperatures remain low enough for snowfall to dominate for longer, and ROS frequencies remain comparatively small even though total precipitation increases.

https://doi.org/10.5194/egusphere-2026-5279
Preprint. Discussion started: 3 September 2026
© Author(s) 2026. CC BY 4.0 License.

The changes are not simply an increase in ROS throughout the cold season. Early in the century, most events between 55°N and 70°N occur in spring, whereas later in the century ROS occurs over a larger part of winter. This is clearest under SSP2-4.5 and SSP5-8.5. The increase in rainfall during March and April is consistent with this shift, since snow is still present over much of the region at this time. At the lower latitudes, however, the spring peak becomes smaller towards the end of the century. Here, further warming begins to shorten the snow season sufficiently that increasing rainfall no longer produces a corresponding increase in ROS. The timing of ROS therefore depends on when rainfall and snow cover coincide, and this period of overlap changes as the climate warms (Peng et al., 2013; López-Moreno et al., 2021).

This also explains some of the differences between the emission pathways. Changes remain relatively small under SSP1-2.6, while SSP2-4.5 shows a clearer extension of ROS into late winter. Under SSP5-8.5, rainfall increases most strongly and the redistribution within the winter season is more pronounced. Yet the high-emission response is not an increase everywhere. The loss of the spring ROS peak at 55-60°N and 60-65°N shows that snow availability becomes a limiting factor in the warmer parts of the study region. Around 65-70°N, snow persists for longer and the late-winter and early-spring signal remains stronger. ROS occurrence is therefore controlled not only by how much rain falls, but also by whether a snowpack is still present when it falls (Cohen et al., 2015). ROS followed by refreezing follows much the same seasonal evolution, although the frequencies are lower. This is expected because the event requires temperatures to fall below 0°C again after rainfall. The reduction in spring events at some latitudes may therefore reflect both earlier snow loss and a decreasing likelihood of freezing conditions following rainfall. This distinction matters for the impacts of ROS: rainfall on snow does not necessarily produce an ice layer, whereas the refreezing subset identifies conditions more directly associated with ice-crust formation.

4.2 Influence of Barents-Kara sea-ice decline

The strong negative correlations between Barents-Kara SIC and precipitation, particularly rainfall, point to a connection between changes over the nearby Arctic seas and winter conditions over land. Declining sea ice exposes larger areas of open water, which can increase heat and moisture exchange with the atmosphere (Vihma, 2014). The strongest rainfall correlations occur during March and April, when precipitation phase is particularly sensitive to temperature, and ROS remains possible over much of the study region. The stronger relationship with rainfall than with total precipitation suggests that changes in precipitation phase may be an important part of this association. Reduced sea ice may also contribute to warmer and more humid air masses reaching northern Fennoscandia, although the pathway linking local ocean conditions to precipitation over land is likely to involve several processes (Ye et al., 2008; Gimeno-Sotelo et al., 2018; Marshall et al., 2020).

The detrended analysis shows that the strong raw correlations partly reflect the long-term changes occurring in both sea ice and precipitation. They do not, however, disappear in all cases. Negative rainfall correlations persist throughout the winter under SSP1-2.6 and SSP2-4.5, and during March and April under all three scenarios. These remaining correlations are weaker, but their persistence during late winter and spring suggests that the shared linear trends do not entirely explain the association. Current and future changes in atmospheric circulation may also contribute to this relationship; Crawford et al. (2023) projected faster and more zonal winter extratropical cyclones over northern Europe under continued warming, which could favour the transport of marine air farther inland. Such changes could occur alongside the increasing open-water area in the Barents and Kara seas and influence winter moisture transport and rainfall. We have not tested this mechanism directly, and temperature, circulation, moisture transport and sea ice are all changing at the same time. The correlations therefore cannot be taken as evidence that sea-ice loss alone drives the precipitation changes over land. Testing this mechanism would require an explicit analysis of atmospheric circulation and moisture transport.

5 Implications

https://doi.org/10.5194/egusphere-2026-5279
Preprint. Discussion started: 3 September 2026
© Author(s) 2026. CC BY 4.0 License.

5.1 Ecosystem impacts

Changes in ROS occurrence, particularly events followed by refreezing, have direct consequences for winter snow conditions. When rain falling on snow is followed by sub-freezing temperatures, ice layers can form within the snowpack or at the ground surface and restrict access to vegetation for grazing animals (Sokolov et al., 2016; Paquotte and Baraer, 2022). As all the reindeer in northern Fennoscandia are privately owned, ROS and extreme precipitation events can be catastrophic for local communities for whom herding constitutes their main livelihood (Laptander et al., 2024). The largest changes in ROS frequency and timing occur between 55°N and 70°N, where reindeer herding is widespread. Changes in seasonality may also be important, as events occurring later in winter or early spring can affect access to forage before snowmelt (Lee et al., 2000). Farther north, where ROS remains less frequent, such impacts are expected to occur less often. The ecological consequences are therefore likely to vary considerably across the region, depending on both the frequency of ROS and whether rainfall is followed by refreezing.

5.2 Implications for human activities and infrastructure

Changes in ROS followed by refreezing also affect conditions relevant to transport and infrastructure. Ice formation at the snow or ground surface can alter road and airstrip conditions and create difficult winter travel conditions, particularly where temperatures fluctuate around freezing (Instanes et al., 2016). The projected redistribution of ROS across a larger part of winter means that these conditions may occur over a broader period than at present. At the same time, the increasing contribution of rainfall to winter precipitation changes snowpack properties and the timing of runoff (Serreze et al., 2021). These changes are relevant for winter transport and water management, especially in areas where seasonal snow cover becomes shorter and less persistent.

5.3 Uncertainty and limitations

The results depend on how well climate models represent precipitation and temperature close to the freezing point. Bias correction reduces systematic model errors, but uncertainty remains in the partitioning of precipitation into rain and snow (McCrystall et al., 2021). ROS events are identified from daily temperature, precipitation and snow-cover conditions, so short rainfall events, diurnal changes in precipitation phase and melt-refreeze cycles cannot be resolved. The use of a threshold to represent snow presence also simplifies changes within the snowpack, and the analysis does not simulate the formation or persistence of individual ice layers.

The relationship between Barents-Kara sea ice and precipitation is another source of uncertainty. Detrending shows that part of the strong raw relationship reflects their common long-term trends, although negative correlations remain for rainfall in several periods, particularly in late winter and early spring. These correlations do not establish a direct causal influence of sea-ice loss on precipitation over land. Atmospheric circulation, moisture transport and temperature can affect both variables, but their individual contributions were not separated in this analysis.

6 Conclusions

Winter precipitation increases across the study region under all three scenarios, together with a progressively larger contribution from rainfall as temperatures rise. This change is greatest under SSP5-8.5 and is accompanied by a redistribution of ROS occurrence within the cold season. Early in the century, ROS events are concentrated mainly in spring between 55°N and 70°N, whereas later in the century they occur over a broader part of winter, particularly under SSP2-4.5 and SSP5-8.5. The response varies with latitude. Around 60-70°N, increasing winter rainfall continues to overlap with an existing snowpack, while farther north colder conditions limit ROS occurrence. At the lower latitudes, the spring ROS peak weakens as snow cover becomes less persistent, showing that increasing rainfall alone does not necessarily lead to more ROS. ROS events followed by refreezing show the same general seasonal

https://doi.org/10.5194/egusphere-2026-5279
Preprint. Discussion started: 3 September 2026
© Author(s) 2026. CC BY 4.0 License.

redistribution but remain less frequent. Barents-Kara sea ice concentration is strongly negatively correlated with land precipitation and, more consistently, with rainfall. Part of this relationship reflects the common long-term trends in sea ice and precipitation, as shown by the weaker correlations after detrending. Nevertheless, negative rainfall correlations remain for the full winter under SSP1-2.6 and SSP2-4.5 and during March and April under all three scenarios. The relationship should therefore be regarded as an association rather than evidence of a direct causal effect of sea-ice loss on precipitation over land. Overall, the results show that future ROS conditions will depend on the changing overlap between winter rainfall, snow persistence and subsequent refreezing, with consequences for snow conditions, ecosystems and human activities across northern Eurasia.

Code availability

The different scripts used to process the CMIP6 data, identify rain-on-snow events and subsequent refreezing, calculate the statistical relationships, and produce the figures are currently being prepared for public release. They are not yet available in a public repository but can be made available to reviewers during the review process. The different scripts will be archived in a public repository before publication, and the corresponding DOI will be added to the revised manuscript.

Data availability

The CMIP6 model data used in this study are publicly available through the Earth System Grid Federation (ESGF). The bias-corrected precipitation and temperature datasets were generated as part of this study and are not currently available in a public repository. The bias-correction procedure used to produce these datasets is described in Sect. 2.3. The datasets can be made available to reviewers during the review process and will be archived in a public repository before publication.

Sea-ice concentration was bias-corrected following the approach described by Crawford and Stroeve (2023). The corresponding bias-corrected CMIP6 sea-ice concentration dataset for the Barents and Kara seas is available through CanWIN at https://doi.org/10.34992/ven0-e283.

Processed data required to reproduce the main analyses and figures will also be made publicly available, with repository information and a persistent identifier added to the manuscript once available.

Author contribution

GV and JS developed the research ideas, GV built the methodology and performed the analysis of the data and the figures, GV and RT bias corrected the CMIP6 temperature/precipitation/snow extent and sea ice concentration, respectively, GV wrote the manuscript with inputs from JS, RT and BCF.

Competing interests

The authors declare that they have no conflict of interest.

© Author(s) 2026. CC BY 4.0 License.

Financial support

This research received funding from the European Union's Horizon 2020 research and innovation programme through the CHARTER project (grant agreement No. 869471, for GV, JS and BCF) and the CRiceS project (grant agreement No. 101003826, for GV and JS), and from the European Union's Horizon Europe programme through the ArcSolution project (grant agreement No. 101135051, for RT). JS and RT were also supported by core AWI funds allocated through the Helmholtz Distinguished Professorship awarded to Julienne Stroeve through the W3 program for the recruitment of leading international female scientists.

References

Adam, J. C., Hamlet, A. F., and Lettenmaier, D. P.: Implications of global climate change for snowmelt hydrology in the twenty-first century, Hydrological Processes: An International Journal, 23(7), 962-972, 2009.

Alexander, L. V., Zhang, X., Peterson, T. C., Caesar, J., Gleason, B., Klein Tank, A. M. G., Haylock, M., Collins, D., Trewin, B., Rahimzadeh, F., Tagipour, A., Rupa Kumar, K., Revadekar, J., Griffiths, G., Vincent, L., Stephenson, D. B., Burn, J., Aguilar, E., Brunet, M., Taylor, M., New, M., Zhai, P., Rusticucci, M., and Vazquez-Aguirre, J. L.: Global observed changes in daily climate extremes of temperature and precipitation, Journal of Geophysical Research: Atmospheres, 111(D5), https://doi.org/10.1029/2005JD006290, 2006.

Barnett, T. P., Adam, J. C., and Lettenmaier, D. P.: Potential impacts of a warming climate on water availability in snow-dominated regions, Nature, 438(7066), 303–309, https://doi.org/10.1038/nature04141, 2005.

Bartsch, A., Kumpula, T., Forbes, B. C., and Stammler, F.: Detection of snow surface thawing and refreezing in the Eurasian Arctic with QuikSCAT: implications for reindeer herding, Ecological Applications, 20(8), 2346-2358, 2010.

Bartsch, A., Bergstedt, H., Pointner, G., Muri, X., Rautiainen, K., Leppänen, L., Joly, K., Sokolov, A., Orekhov, P., Ehrich, D., and Soininen, E. M.: Towards long-term records of rain-on-snow events across the Arctic from satellite data, The Cryosphere, 17, 889-915, https://doi.org/10.5194/tc-17-889-2023, 2023.

Berghuijs, W. R., Woods, R. A., and Hrachowitz, M.: A precipitation shift from snow towards rain leads to a decrease in streamflow, Nature Climate Change, 4(7), 583–586, https://doi.org/10.1038/nclimate2246, 2014.

Bintanja, R., and Andry, O.: Towards a rain-dominated Arctic, Nature Climate Change, 7(4), 263-267, 2017.

Bintanja, R., and Selten, F. M.: Future increases in Arctic precipitation linked to local evaporation and sea-ice retreat, Nature, 509(7501), 479-482, 2014.

Boisvert, L. N., and Stroeve, J. C.: The Arctic is becoming warmer and wetter as revealed by the Atmospheric Infrared Sounder, Geophysical Research Letters, 42(11), 4439-4446, https://doi.org/10.1002/2015GL063775, 2015.

Box, J. E., Colgan, W. T., Christensen, T. R., Schmidt, N. M., Lund, M., Parmentier, F. J. W., Brown, R., Bhatt, U. S., Euskirchen, E. S., Romanovsky, V. E., Walsh, J. E., Overland, J. E., Wang, M., Corell, R. W., Meier, W. N., Wouters, B., Mernild, S., Mård, J., Pawlak, J., and Olsen, M. S.: Key indicators of Arctic climate change: 1971–2017, Environmental Research Letters, 14(4), 045010, https://doi.org/10.1088/1748-9326/aafc1b, 2019.

Cannon, A. J., Sobie, S. R., and Murdock, T. Q.: Bias correction of GCM precipitation by quantile mapping: how well do methods preserve changes in quantiles and extremes?, Journal of Climate, 28(17), 6938-6959, 2015.

Chen, J., Brissette, F. P., Chaumont, D., and Braun, M.: Finding appropriate bias correction methods in downscaling precipitation for hydrologic impact studies over North America, Water Resources Research, 49(7), 4187-4205, 2013.

Cohen, J., Ye, H., and Jones, J.: Trends and variability in rain-on-snow events, Geophysical Research Letters, 42(17), 7115–7122, https://doi.org/10.1002/2015gl065320, 2015.

Crawford, A., and Stroeve, J.: Bias-corrected CMIP6 Daily Sea Ice Concentration in the Barents and Kara Seas [Data set], CanWIN, https://doi.org/10.34992/ven0-e283, 2023.

Crawford, A. D., Lukovich, J. V., McCrystall, M. R., Stroeve, J. C., and Barber, D. G.: Reduced sea ice enhances intensification of winter storms over the Arctic Ocean, Journal of Climate, 35(11), 3353-3370, https://doi.org/10.1175/JCLI-D-21-0747.1, 2022.

Crawford, A. D., McCrystall, M. R., Lukovich, J. V., and Stroeve, J. C.: The response of extratropical cyclone propagation in the Northern Hemisphere to global warming, Journal of Climate, 36, 7123-7142, https://doi.org/10.1175/JCLI-D-23-0082.1, 2023.

Dauginis, A. A., and Brown, L. C.: Recent changes in pan-Arctic sea ice, lake ice, and snow-on/off timing, The Cryosphere, 15(10), 4781-4805, 2021.

Deser, C., Tomas, R., Alexander, M., and Lawrence, D.: The seasonal atmospheric response to projected Arctic sea ice loss in the late twenty-first century, Journal of Climate, 23(2), 333-351, 2010.

DeWalle, D. R., and Rango, A.: Principles of snow hydrology, Cambridge University Press, 2008.

Donat, M. G., Alexander, L. V., Yang, H., Durre, I., Vose, R., and Caesar, J.: Global land-based datasets for monitoring climatic extremes, Bulletin of the American Meteorological Society, 94(7), 997-1006, 2013.

Döscher, R., Vihma, T., and Maksimovich, E.: Recent advances in understanding the Arctic climate system state and change from a sea ice perspective: a review, Atmospheric Chemistry and Physics, 14(24), 13571–13600, https://doi.org/10.5194/acp-14-13571-2014, 2014.

Eyring, V., Bony, S., Meehl, G. A., Senior, C. A., Stevens, B., Stouffer, R. J., and Taylor, K. E.: Overview of the Coupled Model Intercomparison Project Phase 6 (CMIP6) experimental design and organization, Geoscientific Model Development, 9(5), 1937-1958, 2016.

Flato, G., Marotzke, J., Abiodun, B., Braconnot, P., Chou, S. C., Collins, W., Cox, P., Driouech, F., Emori, S., Eyring, V., Forest, C., Gleckler, P., Guilyardi, E., Jakob, C., Kattsov, V., Reason, C., and Rummukainen, M.: Evaluation of climate models, In Climate change 2013: the physical science basis. Contribution of Working Group I to the Fifth Assessment Report of the Intergovernmental Panel on Climate Change (pp. 741-866). Cambridge University Press, https://doi.org/10.1017/CBO9781107415324.020, 2013.

Forbes, B. C., Kumpula, T., Meschtyb, N., Laptander, R., Macias-Fauria, M., Zetterberg, P., Verdonen, M., Skarin, A., Kim, K.-Y., Boisvert, L. N., Stroeve, J. C., and Bartsch, A.: Sea ice, rain-on-snow and tundra reindeer nomadism in Arctic Russia, Biology Letters, 12(11), https://doi.org/10.1098/rsbl.2016.0466, 2016.

Gimeno-Sotelo, L., Nieto, R., Vázquez, M., and Gimeno, L.: A new pattern of the moisture transport for precipitation related to the drastic decline in Arctic sea ice extent, Earth System Dynamics, 9(2), 611–625, https://doi.org/10.5194/esd-9-611-2018, 2018.

Grenfell, T. C., and Putkonen, J.: A method for the detection of the severe rain-on-snow event on Banks Island, October 2003, using passive microwave remote sensing, Water Resources Research, 44(3), 2008.

Gudmundsson, L., Bremnes, J. B., Haugen, J. E., and Engen-Skaugen, T.: Downscaling RCM precipitation to the station scale using statistical transformations–a comparison of methods, Hydrology and Earth System Sciences, 16(9), 3383-3390, 2012.

Hansen, B. B., Isaksen, K., Benestad, R. E., Kohler, J., Pedersen, Å. Ø., Loe, L. E., Coulson, S. J., Larsen, J. O., and Varpe, Ø.: Warmer and wetter winters: characteristics and implications of an extreme weather event in the High Arctic, Environmental Research Letters, 9(11), 114021, https://doi.org/10.1088/1748-9326/9/11/114021, 2014.

Harpold, A. A., Kaplan, M. L., Klos, P. Z., Link, T., McNamara, J. P., Rajagopal, S., Schumer, R., and Steele, C. M.: Rain or snow: hydrologic processes, observations, prediction, and research needs, Hydrology and Earth System Sciences, 21(1), 1-22, https://doi.org/10.5194/hess-21-1-2017, 2017.

Instanes, A., Kokorev, V., Janowicz, R., Bruland, O., Sand, K., and Prowse, T.: Changes to freshwater systems affecting Arctic infrastructure and natural resources, Journal of Geophysical Research: Biogeosciences, 121(3), 567-585, 2016.

IPCC: Climate Change 2021: The Physical Science Basis, Contribution of Working Group I to the Sixth Assessment Report of the Intergovernmental Panel on Climate Change [Masson-Delmotte, V., et al. (eds.)]. Cambridge University Press, https://doi.org/10.1017/9781009157896, 2021.

Kivinen, S., Rasmus, S., Jylhä, K., and Laapas, M.: Long-term climate trends and extreme events in Northern Fennoscandia (1914–2013), Climate, 5(1), 16, 2017.

Knowles, N., Dettinger, M. D., and Cayan, D. R.: Trends in snowfall versus rainfall in the western United States, Journal of Climate, 19(18), 4545-4559, 2006.

Laptander, R., Horstkotte, T., Habeck, J. O., Rasmus, S., Komu, T., Matthes, H., Tømmervik, H., Istomin, K., Eronen, J. T., and Forbes, B. C.: Critical seasonal conditions in the reindeer-herding year: A synopsis of factors and events in Fennoscandia and northwestern Russia, Polar Science, 39, 101016, https://doi.org/10.1016/j.polar.2023.101016, 2024.

Lee, S. E., Press, M. C., Lee, J. A., Ingold, T., and Kurttila, T.: Regional effects of climate change on reindeer: a case study of the Muotkatunturi region in Finnish Lapland, Polar Research, 19(1), 99–105, https://doi.org/10.3402/polar.v19i1.6535, 2000.

López-Moreno, J. I., Pomeroy, J. W., Morán-Tejeda, E., Revuelto, J., Navarro-Serrano, F. M., Vidaller, I., and Alonso-González, E.: Changes in the frequency of global high mountain rain-on-snow events due to climate warming, Environmental Research Letters, 16, 094021, https://doi.org/10.1088/1748-9326/ac0dde, 2021.

Marshall, G. J., Kivinen, S., Jylhä, K., Vignols, R. M., and Rees, W. G.: The accuracy of climate variability and trends across Arctic Fennoscandia in four reanalyses, International Journal of Climatology, 38(10), 3878–3895, https://doi.org/10.1002/joc.5541, 2018.

Marshall, G. J., Jylhä, K., Kivinen, S., Laapas, M., and Dyrrdal, A. V.: The role of atmospheric circulation patterns in driving recent changes in indices of extreme seasonal precipitation across Arctic Fennoscandia, Climatic Change, 162(2), 741–759, https://doi.org/10.1007/s10584-020-02747-w, 2020.

McCabe, G. J., Clark, M. P., and Hay, L. E.: Rain-on-snow events in the western United States, Bulletin of the American Meteorological Society, 88(3), 319-328, 2007.

McCrystall, M. R., Stroeve, J., Serreze, M., Forbes, B. C., and Screen, J. A.: New climate models reveal faster and larger increases in Arctic precipitation than previously projected, Nature Communications, 12(1), 6765, 2021.

Melia, N., Haines, K., and Hawkins, E.: Improved Arctic sea ice thickness projections using bias-corrected CMIP5 simulations, The Cryosphere, 9, 2237-2251, https://doi.org/10.5194/tc-9-2237-2015, 2015.

O'Neill, B. C., Tebaldi, C., van Vuuren, D. P., Eyring, V., Friedlingstein, P., Hurtt, G., Knutti, R., Kriegler, E., Lamarque, J.-F., Lowe, J., Meehl, G. A., Moss, R., Riahi, K., and Sanderson, B. M.: The scenario model intercomparison project

https://doi.org/10.5194/egusphere-2026-5279
Preprint. Discussion started: 3 September 2026
© Author(s) 2026. CC BY 4.0 License.

(ScenarioMIP) for CMIP6, Geoscientific Model Development, 9(9), 3461-3482, https://doi.org/10.5194/gmd-9-3461-2016, 2016.

Pall, P., Tallaksen, L. M., and Stordal, F.: A climatology of rain-on-snow events for Norway, Journal of Climate, 32(20), 6995-7016, 2019.

Paquotte, A., and Baraer, M.: Hydrological behaviour of an ice-layered snowpack in a non-mountainous environment, Hydrological Processes, 36(1), https://doi.org/10.1002/hyp.14433, 2022.

Peng, S., Piao, S., Ciais, P., Friedlingstein, P., Zhou, L., and Wang, T.: Change in snow phenology and its potential feedback to temperature in the Northern Hemisphere over the last three decades, Environmental Research Letters, 8(1), 014008, https://doi.org/10.1088/1748-9326/8/1/014008, 2013.

Putkonen, J., and Roe, G.: Rain-on-snow events impact soil temperatures and affect ungulate survival, Geophysical Research Letters, 30(4), 2003.

Rajulapati, C. R., and Papalexiou, S. M.: Precipitation bias correction: a novel semi-parametric quantile mapping method, Earth and Space Science, 10(4), e2023EA002823, 2023.

Rantanen, M., Karpechko, A. Y., Lipponen, A., Nordling, K., Hyvärinen, O., Ruosteenoja, K., Vihma, T., and Laaksonen, A.: The Arctic has warmed nearly four times faster than the globe since 1979, Communications Earth and Environment, 3, 168, https://doi.org/10.1038/s43247-022-00498-3, 2022.

Rennert, K. J., Roe, G., Putkonen, J., and Bitz, C. M.: Soil thermal and ecological impacts of rain on snow events in the circumpolar Arctic, Journal of Climate, 22(9), 2302-2315, 2009.

Romanovsky, V. E., Smith, S. L., and Christiansen, H. H.: Permafrost thermal state in the polar Northern Hemisphere during the international polar year 2007–2009: a synthesis, Permafrost and Periglacial Processes, 21(2), 106-116, 2010.

Screen, J. A., and Simmonds, I.: The central role of diminishing sea ice in recent Arctic temperature amplification, Nature, 464(7293), 1334-1337, 2010.

Serreze, M. C., and Barry, R. G.: Processes and impacts of Arctic amplification: A research synthesis, Global and Planetary Change, 77(1-2), 85-96, https://doi.org/10.1016/j.gloplacha.2011.03.004, 2011.

Serreze, M. C., Gustafson, J., Barrett, A. P., Druckenmiller, M. L., Fox, S., Voveris, J., Stroeve, J., Sheffield, B., Forbes, B. C., Rasmus, S., Laptander, R., Brook, M., Brubaker, M., Temte, J., McCrystall, M. R., and Bartsch, A.: Arctic rain on snow events: bridging observations to understand environmental and livelihood impacts, Environmental Research Letters, 16(10), 105009, https://doi.org/10.1088/1748-9326/ac269b, 2021.

Smedsrud, L. H., Esau, I., Ingvaldsen, R. B., Eldevik, T., Haugan, P. M., Li, C., Lien, V. S., Olsen, A., Omar, A. M., Otterå, O. H., Risebrobakken, B., Sandø, A. B., Semenov, V. A., and Sorokina, S. A.: The role of the Barents Sea in the Arctic climate system, Reviews of Geophysics, 51(3), 415-449, https://doi.org/10.1002/rog.20017, 2013.

Sokolov, A. A., Sokolova, N. A., Ims, R. A., Brucker, L., and Ehrich, D.: Emergent Rainy Winter Warm Spells May Promote Boreal Predator Expansion into the Arctic, ARCTIC, 69(2), https://doi.org/10.14430/arctic4559, 2016.

Teutschbein, C., and Seibert, J.: Bias correction of regional climate model simulations for hydrological climate-change impact studies: Review and evaluation of different methods, Journal of Hydrology, 456, 12-29, 2012.

Vihma, T.: Effects of Arctic Sea Ice Decline on Weather and Climate: A Review, Surveys in Geophysics, 35(5), 1175–1214, https://doi.org/10.1007/s10712-014-9284-0, 2014.

Walsh, J. E., and Johnson, C. M.: Interannual atmospheric variability and associated fluctuations in Arctic sea ice extent, Journal of Geophysical Research: Oceans, 84(C11), 6915–6928, https://doi.org/10.1029/JC084iC11p06915, 1979.

Ye, H., Yang, D., and Robinson, D.: Winter rain on snow and its association with air temperature in northern Eurasia, Hydrological Processes: An International Journal, 22(15), 2728-2736, 2008.